IJOER
RESEARCH JOURNAL

International Journal of Engineering Research & Science

ISSN
2395-6992

www.ijoer.com
www.adpublications.org

Volume-8! Issue-6! June, 2022

www.ijoer.com ! info@ijoer.com

Preface

We would like to present, with great pleasure, the inaugural volume-8, Issue-6, June 2022, of a scholarly journal, *International Journal of Engineering Research & Science*. This journal is part of the AD Publications series *in the field of Engineering, Mathematics, Physics, Chemistry and science Research Development*, and is devoted to the gamut of Engineering and Science issues, from theoretical aspects to application-dependent studies and the validation of emerging technologies.

This journal was envisioned and founded to represent the growing needs of Engineering and Science as an emerging and increasingly vital field, now widely recognized as an integral part of scientific and technical investigations. Its mission is to become a voice of the Engineering and Science community, addressing researchers and practitioners in below areas

Chemical Engineering	
Biomolecular Engineering	Materials Engineering
Molecular Engineering	Process Engineering
Corrosion Engineering	
Civil Engineering	
Environmental Engineering	Geotechnical Engineering
Structural Engineering	Mining Engineering
Transport Engineering	Water resources Engineering
Electrical Engineering	
Power System Engineering	Optical Engineering
Mechanical Engineering	
Acoustical Engineering	Manufacturing Engineering
Optomechanical Engineering	Thermal Engineering
Power plant Engineering	Energy Engineering
Sports Engineering	Vehicle Engineering
Software Engineering	
Computer-aided Engineering	Cryptographic Engineering
Teletraffic Engineering	Web Engineering
System Engineering	
Mathematics	
Arithmetic	Algebra
Number theory	Field theory and polynomials
Analysis	Combinatorics
Geometry and topology	Topology
Probability and Statistics	Computational Science
Physical Science	Operational Research
Physics	
Nuclear and particle physics	Atomic, molecular, and optical physics
Condensed matter physics	Astrophysics
Applied Physics	Modern physics
Philosophy	Core theories

Chemistry	
Analytical chemistry	Biochemistry
Inorganic chemistry	Materials chemistry
Neurochemistry	Nuclear chemistry
Organic chemistry	Physical chemistry
Other Engineering Areas	
Aerospace Engineering	Agricultural Engineering
Applied Engineering	Biomedical Engineering
Biological Engineering	Building services Engineering
Energy Engineering	Railway Engineering
Industrial Engineering	Mechatronics Engineering
Management Engineering	Military Engineering
Petroleum Engineering	Nuclear Engineering
Textile Engineering	Nano Engineering
Algorithm and Computational Complexity	Artificial Intelligence
Electronics & Communication Engineering	Image Processing
Information Retrieval	Low Power VLSI Design
Neural Networks	Plastic Engineering

Each article in this issue provides an example of a concrete industrial application or a case study of the presented methodology to amplify the impact of the contribution. We are very thankful to everybody within that community who supported the idea of creating a new Research with IJOER. We are certain that this issue will be followed by many others, reporting new developments in the Engineering and Science field. This issue would not have been possible without the great support of the Reviewer, Editorial Board members and also with our Advisory Board Members, and we would like to express our sincere thanks to all of them. We would also like to express our gratitude to the editorial staff of AD Publications, who supported us at every stage of the project. It is our hope that this fine collection of articles will be a valuable resource for *IJOER* readers and will stimulate further research into the vibrant area of Engineering and Science Research.

Mukesh Arora

(Chief Editor)

Board Members

Dr. M. Varatha Vijayan

Annauniversity Rank Holder, Commissioned Officer Indian Navy, Ncc Navy Officer (Ex-Serviceman Navy), Best Researcher Awardee, Best Publication Awardee, Tamilnadu Best Innovation & Social Service Awardee From Lions Club.

Dr. Mohamed Abdel Fatah Ashabrawy Moustafa

PhD. in Computer Science - Faculty of Science - Suez Canal University University, 2010, Egypt.

Assistant Professor Computer Science, Prince Sattam bin AbdulAziz University ALkharj, KSA.

Prof.S.Balamurugan

Dr S. Balamurugan is the Head of Research and Development, Quants IS & CS, India. He has authored/co-authored 35 books, 200+ publications in various international journals and conferences and 6 patents to his credit. He was awarded with Three Post-Doctoral Degrees - Doctor of Science (D.Sc.) degree and Two Doctor of Letters (D.Litt) degrees for his significant contribution to research and development in Engineering.

Dr. Mahdi Hosseini

Dr. Mahdi did his Pre-University (12^{th}) in Mathematical Science. Later he received his Bachelor of Engineering with Distinction in Civil Engineering and later he Received both M.Tech. and Ph.D. Degree in Structural Engineering with Grade "A" First Class with Distinction.

Dr. Anil Lamba

Practice Head – Cyber Security, EXL Services Inc., New Jersey USA.

Dr. Anil Lamba is a researcher, an innovator, and an influencer with proven success in spearheading Strategic Information Security Initiatives and Large-scale IT Infrastructure projects across industry verticals. He has helped bring about a profound shift in cybersecurity defense. Throughout his career, he has parlayed his extensive background in security and a deep knowledge to help organizations build and implement strategic cybersecurity solutions. His published researches and conference papers has led to many thought provoking examples for augmenting better security.

Dr. Ali İhsan KAYA

Currently working as Associate Professor in Mehmet Akif Ersoy University, Turkey.

Research Area: Civil Engineering - Building Material - Insulation Materials Applications, Chemistry - Physical Chemistry – Composites.

Dr. Parsa Heydarpour

Ph.D. in Structural Engineering from George Washington University (Jan 2018), GPA=4.00.

Dr. Heba Mahmoud Mohamed Afify

Ph.D degree of philosophy in Biomedical Engineering, Cairo University, Egypt worked as Assistant Professor at MTI University.

Dr. Dibya Prakash Rai

Post Doctoral Fellow (PDF), M.Sc., B.Sc., Working as Assistant Professor in Department of Physics in Pachhuncga University College, Mizoram, India.

Dr. Pankaj Kumar Pal

Ph.D R/S, ECE Deptt., IIT-Roorkee.

Dr. P. Thangam

PhD in Information & Communication Engineering, ME (CSE), BE (Computer Hardware & Software), currently serving as Associate Professor in the Department of Computer Science and Engineering of Coimbatore Institute of Engineering and Technology.

Dr. Pradeep K. Sharma

PhD., M.Phil, M.Sc, B.Sc, in Physics, MBA in System Management, Presently working as Provost and Associate Professor & Head of Department for Physics in University of Engineering & Management, Jaipur.

Dr. R. Devi Priya

Ph.D (CSE), Anna University Chennai in 2013, M.E, B.E (CSE) from Kongu Engineering College, currently working in the Department of Computer Science and Engineering in Kongu Engineering College, Tamil Nadu, India.

Dr. Sandeep

Post-doctoral fellow, Principal Investigator, Young Scientist Scheme Project (DST-SERB), Department of Physics, Mizoram University, Aizawl Mizoram, India- 796001.

Dr. Roberto Volpe

Faculty of Engineering and Architecture, Università degli Studi di Enna "Kore", Cittadella Universitaria, 94100 – Enna (IT).

Dr. S. Kannadhasan

Ph.D (Smart Antennas), M.E (Communication Systems), M.B.A (Human Resources).

Research Area: Engineering Physics, Electromagnetic Field Theory, Electronic Material and Processes, Wireless Communications.

Mr. Amit Kumar

Amit Kumar is associated as a Researcher with the Department of Computer Science, College of Information Science and Technology, Nanjing Forestry University, Nanjing, China since 2009. He is working as a State Representative (HP), Spoken Tutorial Project, IIT Bombay promoting and integrating ICT in Literacy through Free and Open Source Software under National Mission on Education through ICT (NMEICT) of MHRD, Govt. of India; in the state of Himachal Pradesh, India.

Mr. Tanvir Singh

Tanvir Singh is acting as Outreach Officer (Punjab and J&K) for MHRD Govt. of India Project: Spoken Tutorial - IIT Bombay fostering IT Literacy through Open Source Technology under National Mission on Education through ICT (NMEICT). He is also acting as Research Associate since 2010 with Nanjing Forestry University, Nanjing, Jiangsu, China in the field of Social and Environmental Sustainability.

Mr. Abilash

MTech in VLSI, BTech in Electronics & Telecommunication engineering through A.M.I.E.T.E from Central Electronics Engineering Research Institute (C.E.E.R.I) Pilani, Industrial Electronics from ATI-EPI Hyderabad, IEEE course in Mechatronics, CSHAM from Birla Institute Of Professional Studies.

Mr. Varun Shukla

M.Tech in ECE from RGPV (Awarded with silver Medal By President of India), Assistant Professor, Dept. of ECE, PSIT, Kanpur.

Mr. Shrikant Harle

Presently working as a Assistant Professor in Civil Engineering field of Prof. Ram Meghe College of Engineering and Management, Amravati. He was Senior Design Engineer (Larsen & Toubro Limited, India).

Zairi Ismael Rizman

Senior Lecturer, Faculty of Electrical Engineering, Universiti Teknologi MARA (UiTM) (Terengganu) Malaysia Master (Science) in Microelectronics (2005), Universiti Kebangsaan Malaysia (UKM), Malaysia. Bachelor (Hons.) and Diploma in Electrical Engineering (Communication) (2002), UiTM Shah Alam, Malaysia.

Mr. Ronak

Qualification: M.Tech. in Mechanical Engineering (CAD/CAM), B.E.

Presently working as a Assistant Professor in Mechanical Engineering in ITM Vocational University, Vadodara. Mr. Ronak also worked as Design Engineer at Finstern Engineering Private Limited, Makarpura, Vadodara.

Table of Contents

Volume-8, Issue-6, June 2022

S. No	Title	Page No.
1	**New Low-Potential Heat Exchangers Design** **Authors:** Mária Čarnogurská, Róbert Gallik, Miroslav Příhoda **DOI:** https://dx.doi.org/10.5281/zenodo.6775378 **Digital Identification Number:** IJOER-JUN-2022-2	01-05
2	**Theory of Spin Waves in a Thin Ferromagnetic Film with a Periodic System of Circular Antidots. Solutions that Correspond to the Crystal Band Theory** **Authors:** V.V. Kulish **DOI:** https://dx.doi.org/10.5281/zenodo.6775416 **Digital Identification Number:** IJOER-JUN-2022-5	06-12

New Low-Potential Heat Exchangers Design

Mária Čarnogurská[1*], Róbert Gallik[2], Miroslav Příhoda[3]

[1,2]Department of Power Engineering, Faculty of Mechanical Engineering, Technical University of Košice, 042 00 Košice, Slovak Republic.

[3]Department of Thermal Engineering, Faculty of Materials Science and Technology, VSB –Technical University of Ostrava, 708 33 Ostrava-Poruba, Czech Republic.

*Corresponding Author

Received: 02 June 2022/ Revised: 12 June 2022/ Accepted: 19 June 2022/ Published: 30-06-2022

Abstract— *This article deals with the effects of different structural arrangements inside a heat exchanger made of polypropylene tubes on the overall heat transfer coefficient. The experiments indicated that overall heat transfer coefficient k with stretched tubes was lower than the value observed when the tubes were slightly loosened. Tubes should not be loosened by more than 5 % of their length. If this value is exceeded, tubes may accumulate near the wall and their contact with water is insufficient; this results in reduced heat transfer. Equally important is to prevent tubes from attaching to each other. This may be achieved with a variety of turbulators. A turbulator may be any small object, metal or plastic, which is inserted among the tubes. Laboratory investigation indicated that turbulators can increase overall heat transfer coefficient by as much as 54 %compared to heat exchangers without turbulators, in identical operating conditions.*

Keywords— ***Heat exchanger, atypical structure, polypropylene tube, turbulators.***

I. INTRODUCTION

Heat exchangers which are primarily intended for the use with low-potential heat sources have been described in paper [1]. Heat-transfer surfaces in such heat exchangers are on polypropylene tubes and they may be either absolutely smooth and gas-proof or porous. Polypropylene tubes in these exchanges are hollow. A required amount of tube ends are sealed into a polyurethane tube approximately 35 mm long to form a potting. A fluid (water) which absorbs heat from the surrounding environment (a low-potential heat source) flows through these tubes sealed in the potting. An identical potting is on the outflow end of the heat exchanger. A length of tubes between the pottings ranges from approximately 400 mm to max. 1,000 mm. A heat-transfer surface area *S* is calculated using the amount and dimensions of the used tubes and it determines the heat output of a heat exchanger. An inner diameter of a capillary tube usually ranges between approximately 0.15 and0.30 mm. Heat exchangers of this type, with simple designs, have been subjected to experimental research aimed at obtaining information on the overall heat transfer coefficient *k*, as presented in the quoted literature.

The heat exchangers presented in this article consisted of the same tubes as described above, but with a special feature, i.e. the arrangement of tubes between the two pottings. The article describes an analysis of three different designs of a heat exchanger.

II. SHELL AND TUBE HEAT EXCHANGER

A heat exchanger of this type consisted of a cylindrical shell with a diameter of 60 mm. The shell was made of a PVC tube (Fig. 1). Both tube ends (2) contained a sealed-in potting of capillary tubes (1). The tubes inside the shell were arranged so that they crossed the baffles. The purpose of the ring-shaped baffles (3) was to direct the fluid stream into the tube bundle and across the whole heat exchanger. The baffles were designed so that all tubes in the bundle are evenly distributed along their outer circumference and that a baffle gently pushes the tubes against the inner wall of the heat exchanger shell. The fluid stream had to cross the freely placed tubes in order to return to the axis of the heat exchanger. The same principle was applied to the installation of the smaller ring-shaped baffles (4). Their purpose was again to ensure that the tubes are evenly distributed along their circumference. These smaller baffles were also intended to push the fluid stream away from the heat exchanger axis towards the walls; therefore, the stream had to cross the tubes in the bundle again. The effect of alternating positions of the small and large baffles was that the stream repeatedly crossed the tubes. The baffles were made of toughened polystyrene and the tubes were attached to them with silicone seal and water-proof sealing tape.

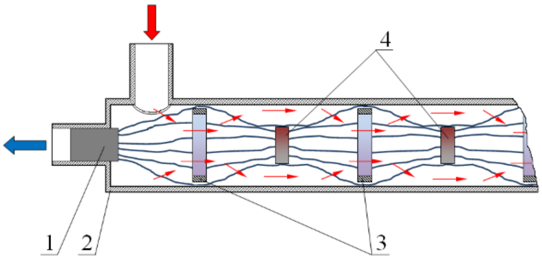

FIGURE 1: Shell and tube heat exchanger

The red arrows in Fig. 1 indicate the fluid stream flowing around the tubes and the blue arrow indicates the fluid stream flowing though the tubes. Fig. 2 shows a tube bundle with all baffles glued to it and Fig. 3 shows a detail of a small and a large baffle. The tube bundle with such an arrangement was inserted into a cylindrical body of a heat exchanger. To avoid damage to the baffles during insertion, the body was heated in a water bath to the temperature of 80 °C and the tube bundle was cooled to the temperature of 5 °C. This was carried out while using a relatively high expansibility of the used plastic materials. The parameters of the experimentally examined shell and tube heat exchanger are listed in Table. 1.

FIGURE 2: The adjusted bundle

FIGURE 3: A detail of the inner and outer baffles

TABLE 1
PARAMETERS OF THE SHELL AND TUBE HEAT EXCHANGER

Number of tubes	1,400 pieces	**Outer diameter of the tube**	0.275 mm
Tube length	550 mm	**Heat-transfer surface area**	0.665 m^2

During the experiment, the heat exchanger was in operation for approximately 10 minutes in a horizontal position. The obtained values of the parameters, which were necessary to calculate overall heat transfer coefficient k at a flow rate of fluid inside the tubes was V_{in} = 200 L·hr^{-1}, were used to plot a curve of a correlation between the overall heat transfer coefficient k and the time τ (Fig. 4).

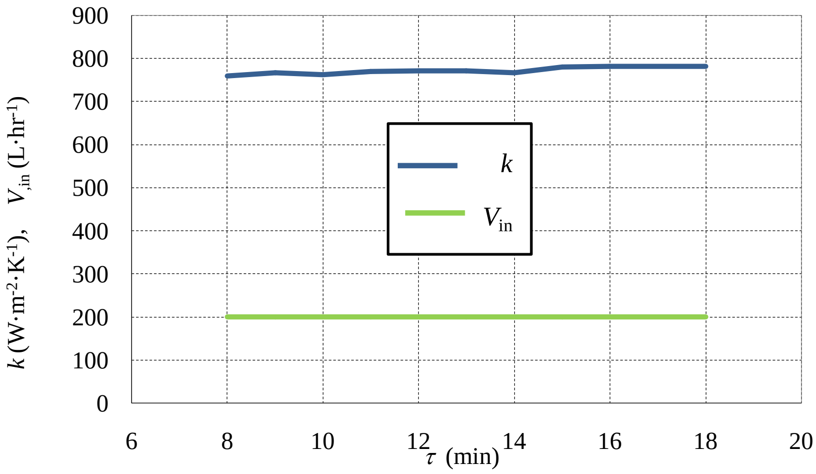

FIGURE 4: Overall heat transfer coefficient for a shell and tube heat exchanger

A maximum mean value of overall heat transfer coefficient k was 780 $W \cdot m^{-2} \cdot K^{-1}$. The method used for expressing this parameter is described in detail in paper [1]. Due to the fact that the obtained values of overall heat transfer coefficient were low, no further measurements were carried out on this type of heat exchanger.

III. HEAT EXCHANGER WITH TURBULATORS IN THE TUBE BUNDLE

In this type of heat exchanger, turbulators were inserted into the tube bundle. Turbulators were various small metal and plastic objects (nuts, bolts etc.). A detailed image of the bundle adjusted as described above is shown in Fig. 5. Parameters of the examined tube bundle are listed in Table2.

TABLE 2
PARAMETERS OF HEAT EXCHANGER WITH TURBULATORS

Number of tubes	1,400 pieces	**Outer diameter of the tube**	0.275 mm
Tube length	680 mm	**Heat-transfer surface area**	0.68 m^2

An inlet of the low-potential fluid into the heat exchanger was tangential (a yellow arrow in Fig. 6). During the experiment, the heat exchanger was positioned vertically.

FIGURE 5: A detailed image of turbulators

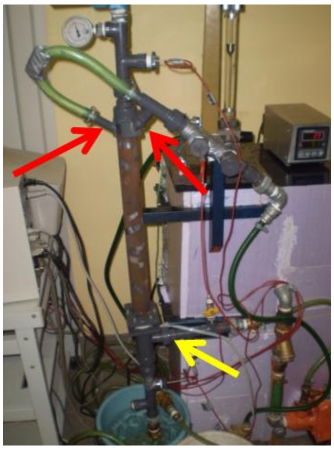

FIGURE 6: Heat exchanger arrangement during the experiment

Prior to the experiment, the tubes in the heat exchanger were loosened by3.7 %. This means that a tube with a length of 680 mm (Table 2) was placed inside a cylindrical shell of the heat exchanger with a length of only 655 mm. The overall heat transfer coefficient k was identified while applying the same method as before, as described in paper [1]. During the experiment, a flow rate of the fluid inside the tubes V_{in} was increased from 30 $L \cdot hr^{-1}$to 200 $L \cdot hr^{-1}$. The heat exchanger was in operation in a vertical position. The fluid exited the heat exchanger through two tangential outlets (red arrows in Fig. 6). The curve of a correlation between the overall heat transfer coefficient and the flow rate inside the tubes V_{in} is shown in Fig. 7.

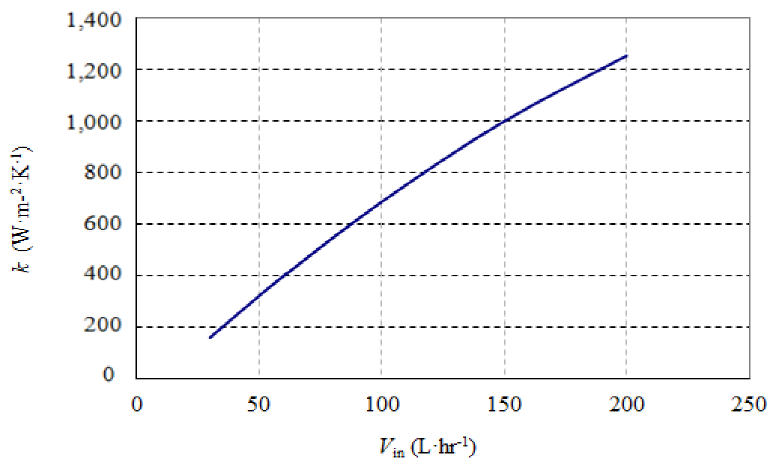

FIGURE 7: Overall heat transfer coefficient for heat exchanger with turbulators in the tube bundle

The curve indicates that optimal loosening of the tubes in the bundle and the use of turbulators may facilitate achieving a value of overall heat transfer coefficient as much as 1,200 $W{\cdot}m^{-2}{\cdot}K^{-1}$.

IV. HEAT EXCHANGER WITH TUBES WITH HINDERED TRANSVERSE MOTIONS

Laboratory tests were also performed with heat exchangers which were filled up with tubes so that their transverse motions were impossible. The body of such exchangers was made of a PVC tube. Parameters of the tested heat exchanger are listed in Table 3. The inner diameter of the PVC tube in this heat exchanger was 25 mm, and the number of tubes inside was 400. As the whole flow cross-section of the heat exchanger was filled up with tubes, the motions of the tubes were significantly hindered. The inlet and outlet for the fluid (low-potential water) were tangential (yellow arrows in Fig. 8). Therefore, in the heat exchanger with the parameters specified in Table 3, the fluid flew around the tubes in an oblique, lengthwise direction.

FIGURE 8: Heat exchanger with tubes with hindered transverse motions

TABLE 3
PARAMETERS OF HEAT EXCHANGER V001

Number of tubes	400 pieces	Outer diameter of the tube	0.6 mm
Tube length	260 mm	Heat-transfer surface area	0.196 m^2

The tubes in the bundle were loosened before they were sealed in a potting. Due to a diameter of the tubes, the loosening rate was only 0.5 %. This procedure was based on the knowledge obtained in experiments with a heat exchanger with turbulators. The temperature of fluid entering the heat exchanger was 50 °C. Flow rates inside the tubes were of three different values (150 $L{\cdot}hr^{-1}$, 300 $L{\cdot}hr^{-1}$ and 600 $L{\cdot}hr^{-1}$).A decisive factor was the flow rate of the fluid flowing outside the tubes, which amounted to950 $L{\cdot}hr^{-1}$ and 1,200 $L{\cdot}hr^{-1}$. Measurements were also made for a pressure drop in the heat exchanger; the measured values ranged from 30 to 150 kPa, depending on the flow rate (Fig. 9). Increased flow rates were reflected in increased values of overall heat transfer coefficient *k*, with a maximum value of 1,875 $W{\cdot}m^{-2}{\cdot}K^{-1}$. With regard to the fact that the fluid used in the experiment was pure water, such a value of overall heat transfer coefficient will not be feasible in real conditions. Water that will enter a heat exchanger will be polluted; therefore, there will have to be some free space among the tubes to avoid clogging of the heat exchanger with impurities, as this would reduce the *k* value.

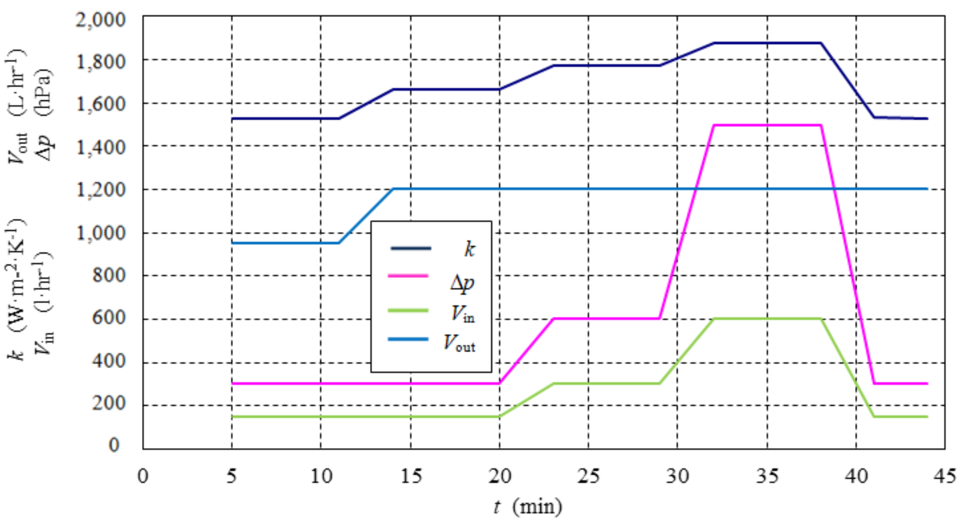

FIGURE 9: Values of overall heat transfer coefficient *k* and pressure drop Δp at different flow rates inside the tubes V_{in} and around the tubes V_{out}

V. CONCLUSION

The article describes three different designs of heat exchangers made of propylene capillary tubes. Results of this experimental laboratory investigation indicated that the most optimal design of a heat exchanger for achieving maximum values of overall heat transfer coefficient is the heat exchanger with tubes that are prevented from transverse motions and only slightly loosened (max 0.5 %). This type of heat exchanger meets the requirement of providing sufficient heat transfer from a heat-transfer fluid. However, it is necessary to bear in mind that these experiments were carried out with pure water. With polluted water, it is necessary to count with reduced amounts of transferred heat. In this investigation, with pure water, a maximum heat output of the heat exchanger was 4,450 W.

ACKNOWLEDGEMENTS

This paper was written with the financial support of the granting agency VEGA within the project 1/0626/20, project 1/0532/22 and from FMT VŠB-TUO within the project SP 2022/13.

REFERENCES

[1] M. Čarnogurská, R. Gallik, Non-typical designs of Polypropylene Capillary Heat Exchangers, In: International Journal of Engineering Research and Science = IJOER. vol. 7, no. 1 (2021), pp. 1-4.

[2] D. M. Zarkadas, K. K. Sirkar, Polymeric Hollow Fiber Heat Exchangers: An Alternative for Lower. Temperature Applications. In Eng. Chem. Res., vol. 43, 2004, pp. 8093-8106.

[3] M. Čarnogurská, M. Příhoda, M. Lázár, N. Jasminská, R. Gallik, M. Kubík, Measuring Selected Parameters of Polypropylene Fibre Heat Exchangers. Strojniskivestnik, vol. 62, no. 6, (2016), pp.381-384.

[4] L. Jachuck, R. J. J. Zaheed, Review of polymer compact heat exchangers, with special emphasis on a polymer film unit. In Applied Thermal Engineering, vol. 24, 2004, no 16, pp. 2323-2358.

[5] R. Gallik, M. Dohnal, Potted sets of hollow fibers as low cost heat exchangers. (in Slovak). SROJÁRSTVO/SROJÍRENSTVÍ, (special edition). 2009, pp. 61-62.

[6] M. Čarnogurská, R. Gallik, Výmenníky tepla na báze polypropylénu. Plynár-Vodár-Kúrenár + Klimatizácia. (in Slovak). 1-2/2021, pp. 27-30.

Theory of Spin Waves in a Thin Ferromagnetic Film with a Periodic System of Circular Antidots. Solutions that Correspond to the Crystal Band Theory

V.V. Kulish

Department of general physics, National Technical University of Ukraine "Igor Sikorsky Kyiv Polytechnic Institute", 37 Peremogy prosp., 03056, Kyiv, Ukraine

Received: 10 June 2022/ Revised: 16 June 2022/ Accepted: 22 June 2022/ Published: 30-06-2022

Abstract— *The paper continues study of dipole-exchange spin waves in a two-dimensional magnonic crystal (a thin ferromagnetic film with a periodic system of circular antidots) started by the author in the previous paper. The proposed model considers the magnetic dipole-dipole interaction, the exchange interaction and the anisotropy effects. An improved method of obtaining the dispersion relation as well as the values' spectra of the frequencies and wavenumbers for the investigated spin waves – the method based on using the Bloch-type solutions of the Landau-Lifshitz equation for the spin waves together with the Born–von Karman boundary conditions – is proposed. Exploitation of the above-mentioned method essentially extends the area of application of the obtained results compared to the previous paper. Newly obtained spectral characteristics are shown to exhibit crystal-type band structure with band gaps. The wave vector component that correspond to the wave propagating orthogonally to the film plane is shown to have narrow allowed bands, so its values' spectrum is near discrete.*

Keywords— Magnetic dynamics, Spin wave, Dipole-exchange theory, Ferromagnetic antidot, Magnonic crystal.

I. INTRODUCTION

Spin waves in nanosystems become an actual and promising topic of research because of their numerous applications - both current and prospective - in different fields of technology. These applications include mostly new devices for data storage, transfer and processing [1-4]. Such applications require precise theoretical models of excitation and propagation of spin waves in nanosystems of different configurations, thus causing these models to be extensively developed recently.

Prospective materials for applications in spin-wave technologies include, in particular, magnonic crystals [5,6] - composite materials whose magnetic properties change periodically along one, two or three directions. They are known to exhibit unique magnetic properties [5] making them prospective for creating novel magnonic devices [5,6]. As a result, spin waves in magnonic crystals of different configurations are studied extensively, both theoretically and experimentally [7-9].

Because of the parameters' periodicity, magnonic crystals often exhibit properties similar to those observed in crystals, such as appearance of crystal-like band structure in the spin waves' spectrum (see, e.g., [8]). Therefore, elements of crystals theory can be used in a theory of spin waves in such nanosystems in order to refine corresponding models and, therefore, obtain more precise results.

The paper extends theoretical study of dipole-exchange spin waves in a two-dimensional magnonic crystal (a thin ferromagnetic film with a two-dimensional periodic system of circular antidots) started by the author in the previous paper [10].The magnetic dipole-dipole interaction, the exchange interaction and the anisotropy effects are considered. Unlike in the previous paper, periodicity of the system is taking into account by applying the Bloch theorem and using the Bloch-type solutions of the Landau-Lifshitz equations for a spin wave together with Born–von Karman boundary condition. As a result, a refined dispersion relation and the wave vector components' spectrum of such waves is obtained. Analysis shows that a crystal-type band structure with band gaps appears in the resulting spectral characteristics.

II. PROBLEM STATEMENT: MODEL DESCRIPTION

Let us consider a ferromagnetic film with the thickness l composed of a uniaxial ferromagnet of the "easy axis" type containing a periodic two-dimensional system of identical circular antidots with the distances between the centers of neighboring antidots a and the radii R (see Fig. 1). Let us denote the ferromagnet parameters as follows: the exchange constant α, the uniaxial anisotropy parameter β (is considered constant), the gyromagnetic ratio γ (is considered constant). The easy magnetization axis of the ferromagnet (and hence the ground state magnetization $\vec{M}_0$, which is considered constant in the entire volume of the film) is directed orthogonally to the film and the Oz axis is chosen in this direction. The external magnetic field $\vec{H}_0^{(e)}$ is assumed to be homogeneous and directed along the Oz axis.

If the film is thin enough or the outer field is strong enough ($l \sim l_{ex}$ where l_{ex} is the exchange length of the ferromagnet, $l<<R$ or $H_0^{(e)} >> 4\pi M_0$), the ground state magnetization vector has an approximately uniform distribution, and the internal magnetic field of the film is also directed along the Oz axis and is approximately equal to the field inside a continuous film (without antidots) subjected to the same external magnetic field: $\vec{H}_0^{(i)} \approx \vec{H}_0^{(e)} - 4\pi\vec{M}_0$. (To be exact, the condition of the film thinness compared to the characteristic size of the antidot system should include not the antidot radius R, but the minimal distance d=2(a –R) between the antidots: $l<<d=2(a-R)$).

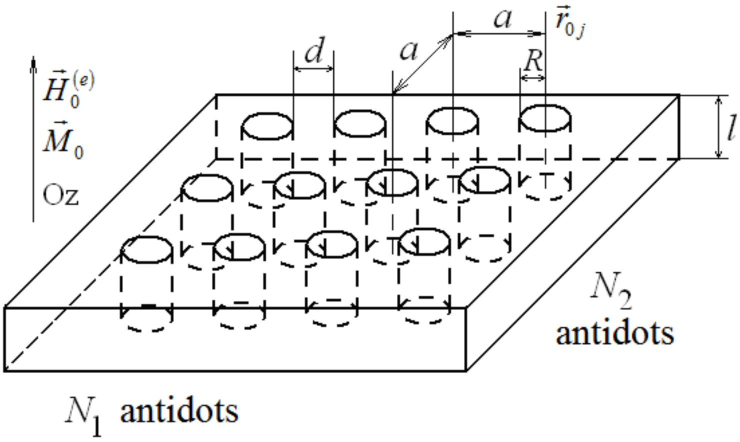

FIGURE 1: The considered antidot system.

Note that such system can be considered as an example of a two-dimensional magnonic crystal as its magnetic properties change periodically along 2 dimensions.

Let us consider a spin wave propagating in the above-described film and take into account both the magnetic dipole-dipole and exchange interaction as well as the anisotropy in the Landau-Lifshitz equation. The wave is considered linear so that the magnetization $\vec{m}$ and the magnetic field $\vec{h}$ of the wave are small perturbations of the overall magnetization $\vec{M}$ and the magnetic field inside the ferromagnet $\vec{H}^{(i)}$, correspondingly. Thus, the relations $|\vec{m}| << |\vec{M}_0|$, $|\vec{h}| << |\vec{H}_0^{(i)}|$ fulfill, where $\vec{H}_0^{(i)}$ is the ground state internal magnetic field (so that $\vec{M} = \vec{M}_0 + \vec{m}$, $\vec{H}^{(i)} = \vec{H}_0^{(i)} + \vec{h}$).

Let us note that the spin wave pattern in the system depends significantly on the minimum distance between adjacent antidots d. From the properties of the exchange length l_{ex} implies the fact that when $d< l_{ex}$, the studied system actually splits into a system of separate magnetic quantum dots and the spin wave propagates in directions orthogonal to vectors that connect neighboring antidots and in narrow adjacent sectors. Let us investigate spin waves in the system for the case $d>> l_{ex}$, so that these spin waves can be described similarly to spin waves in a continuous film. The task of the paper is to find the dispersion relation, the wavenumber values' spectrum and the frequency values' spectrum for the above-described spin waves.

A linearized Landau-Lifshitz equation (see, e.g., [11]) for such film together with the Maxwell equation $div\vec{h} = -4\pi \cdot div\vec{m}$ in a magnetostatic approximation (see, e.g., [11]) – where $\vec{h}$ is an internal magnetic field perturbation and $\vec{m}$ is a magnetization perturbation – forms a system of equations in which the spin wave magnetization vector can be eliminated. Therefore, the following equation for the amplitude Φ_0 of the magnetic potential Φ (so that $\Phi = \Phi_0 \exp(i\omega t)$) can be obtained:

$$\left(\frac{\omega^2}{\gamma^2 M_0^2}-\left(\frac{H_0^{(i)}}{M_0}+\beta-\alpha\Delta\right)\left(\left(\frac{H_0^{(i)}}{M_0}+\beta\right)+4\pi-\alpha\Delta\right)\right)\Delta\Phi_0+4\pi\left(\frac{H_0^{(i)}}{M_0}+\beta-\alpha\Delta\right)\frac{\partial^2\Phi_0}{\partial z^2}=0 \quad (1)$$

here ω is the spin wave frequency (see, e.g., [10]).

III. SPECTRAL CHARACTERISTICS OF THE SPIN WAVES

First, similarly to [10] let us seek a solution of (1) that corresponds to the system symmetry. After choosing the orthogonal (in-plane) part of the solution in the form of a combination of the Bessel and Neumann functions and considering the system symmetry relative to the rotation transformation one can obtain:

$$\Phi_{sym}=\exp(-i\omega t)\left(\Gamma_1\cos(k_{||}z)+\Gamma_2\sin(k_{||}z)\right)\sum_{j,n}\left(A_n J_{4n}\left(k_\perp\left|\vec{r}_\perp-\vec{r}_{0j}\right|\right)+B_n N_{4n}\left(k_\perp\left|\vec{r}_\perp-\vec{r}_{0j}\right|\right)\right)\exp\left(4in\theta_j\right) \quad (2)$$

here the radius vector $\vec{r}_\perp$ lies in the plane normal to $\vec{M}_0$ (xOy plane), j is the antidot number, θ_j is the polar angle measured from the center of the antidot number j, $k_\perp$ and $k_{||}$ are the wavenumbers that correspond to propagation of the spin wave in the plane xOy and in the ortogonal direction, correspondingly, J_n and N_n are the Bessel and Neumann functions of the order n, correspondingly, while Γ_1, Γ_2, A_n and B_{jn} are constants. For every wave that enters the superposition (2) (and, therefore, for the entire superposition (2)) the Laplace equation $\Delta\Phi_{sym}=-\left(k_\perp^2+k_{||}^2\right)\Phi$ fulfills. After substituting this solution into the equation (1), one can obtain a dispersion relation (presented in [10]).

Now, let us take advantage of the fact that the considered system possesses space periodicity, so conditions of the Bloch theorem formally fulfill for the equation (1). Therefore, its solution can be chosen as a combination of the Bloch-type functions for the magnetic potential. Such solution can be written in the form $\Phi(\vec{r},t)=\exp(-i\omega t)\Phi_0(\vec{r})$ with the following expression for Φ_0:

$$\Phi_0=\left(\Gamma_1\cos(k_{||}z)+\Gamma_2\sin(k_{||}z)\right)\Phi_{0\perp}(\kappa,\vec{r}_\perp)=\left(\Gamma_1\cos(k_{||}z)+\Gamma_2\sin(k_{||}z)\right)\exp\left(i\vec{k}_\perp'\vec{r}_\perp\right)F_{per}\left(\vec{k}_\perp,\vec{r}_\perp\right) \quad (3)$$

where $\vec{k}_\perp$ and $\vec{k}_\perp'$ are in-plane wave vectors ($\vec{k}_\perp$ corresponds to the symmetrical solution), κ is a total in-plane wavenumber and the relation $\Delta_\perp\Phi_{0\perp}=-\kappa^2\Phi_{0\perp}$ (where the operator $\Delta_\perp=\partial^2/\partial x^2+\partial^2/\partial y^2$) fulfills. The function F_{per} has in-plane periodicity - but nevertheless, substitution of $\Phi_{0\perp}$ into the relation $\Delta_\perp\Phi_{0\perp}=-\kappa^2\Phi_{0\perp}$ shows that the function F_{per} doesn't coincide with the corresponding function in (2). After substituting (3) into (2) one can obtain the following dispersion relation:

$$\omega=\gamma M_0\sqrt{\alpha^2k^4+2\alpha\left(2\pi+\tilde{\beta}\right)k^2+\tilde{\beta}\left(4\pi+\tilde{\beta}\right)-4\pi k_{||}^2\left(\alpha+\frac{\tilde{\beta}}{k^2}\right)} \quad (4)$$

where $\tilde{\beta}=H_0^{(i)}/M_0+\beta$ (so for the considered thin film $\tilde{\beta}\approx\beta+\left(H_0^{(e)}-4\pi M_0\right)/M_0=\beta-4\pi+H_0^{(e)}/M_0$) and the total wavenumber $k^2=\kappa^2+k_{||}^2$. The dispersion relation is expressed by a formula similar to the one obtained in [10], however, an expression for the total wavenumber k that enters these dispersion relations differ and moreover, the parameter κ that enters k depends on both $\vec{k}_\perp$ and $\vec{k}_\perp'$ for Bloch-type solutions, thus making these dispersion relations essentially different.

As the wave vector of the investigated spin waves has both longitudinal and orthogonal components, for more complete specification of the spin wave pattern the dispersion relation (4) must be supplemented by either a spectrum of values of at least one of these components or a relation between them. The spectrum of values of the longitudinal wave number can be found from the condition of limited film thickness, of the orthogonal wave number - either from the periodicity feature of the system or from boundary conditions.

The cylindrical functions that enter (2) are not periodical, but they asymptotically tend to periodical functions when the distance to the chosen central antidot increases (see [10]). As the considered system possess the translational symmetry, the resulting harmonical functions' phase change on the translation period of the system should be a multiple of 2π. The same considerations can be applied to the symmetrical part of the Bloch-type solutions (3) regardless of the exact form of the function F_{per}. Therefore, the "symmetrical" orthogonal wavenumber $k_\perp$ should have the same form as the single orthogonal wavenumber found in [10]:

$$k_\perp(s) = \frac{2\pi s}{a} \tag{5}$$

with $s \in \aleph \cup \{0\}$ being a number of the orthogonal mode. As the film is considered large (in Ox and Oy directions) and the total antidot number is considered big, spectral characteristics of the spin wave should not be sensitive to the exact form of boundary conditions, so Born–von Karman boundary conditions from the crystal electronic band theory can be used. Let us choose the ferromagnetic film to be a rectangle whose sides are parallel to the Ox and Oy axes and contain N_1 antidots along the Ox axis, N_2 antidots along the Oy axis. Then, using two-dimensional Born–von Karman boundary conditions at the boundaries of the rectangle, one can obtain $\vec{k}_\perp' = \frac{2\pi}{aN_1} q_1 \vec{e}_x + \frac{2\pi}{aN_2} q_2 \vec{e}_y$, where q_1 and q_2 are arbitrary integers. To obtain the total in-plane wavenumber κ, let us expand the function F_{per} into the Fourier series: $F_{sym}(\vec{r}_\perp) = \sum_{\vec{K}_\perp} A_{\vec{K}_\perp} \exp(i\vec{K}_\perp \vec{r}_\perp)$, where $\vec{K}_\perp = \frac{2\pi}{a} p_1 \vec{e}_x + \frac{2\pi}{a} p_2 \vec{e}_y$ are the reciprocal lattice vectors (p_1, p_2 are arbitrary integers). After substituting F_{per} in this form into the $\Delta_\perp \Phi_{0\perp} = -\kappa^2 \Phi_{0\perp}$ one can obtain the expression known from the theory of crystal solids $\kappa^2 = \left(\vec{K}_\perp + \vec{k}_\perp'\right)^2$. Therefore, the sought spectrum of values of can be written as follows:

$$\kappa^2 = \left(\frac{2\pi}{a}\right)^2 \left(\left(p_1 + \frac{q_1}{N_1}\right)^2 + \left(p_2 + \frac{q_2}{N_2}\right)^2 \right) \tag{6}$$

After applying the standard magnetic boundary conditions together with the magnetic potential continuity condition (that should be applied twice - on the film boundary and on the antidots' boundaries) and substituting the solutions of the Laplace equations for the magnetic potential outside the film and inside the antidots, after some transformations one can obtain $\kappa = k_{||} \mathrm{tg}(k_{||} l/2)$, $\Gamma_1 \Gamma_2 = 0$. Therefore, the spin wave frequencies' spectrum is determined implicitly by the following system of conditions:

$$\left\{ \begin{array}{l} \omega(p_1, p_2, q_1, q_2, k_{||}) = \gamma M_0 \sqrt{\begin{array}{l} \alpha^2 \left(k_{||}^2 + \left(\frac{2\pi}{a}\right)^2 \left(\left(p_1 + \frac{q_1}{N_1}\right)^2 + \left(p_2 + \frac{q_2}{N_2}\right)^2 \right) \right)^2 + \\ + 2\alpha\left(2\pi + \tilde{\beta}\right) \left(k_{||}^2 + \left(\frac{2\pi}{a}\right)^2 \left(\left(p_1 + \frac{q_1}{N_1}\right)^2 + \left(p_2 + \frac{q_2}{N_2}\right)^2 \right) \right) + \tilde{\beta}\left(4\pi + \tilde{\beta}\right) - \\ - 4\pi k_{||}^2 \left(\alpha + \frac{\tilde{\beta}}{k_{||}^2 + (2\pi/a)^2 \left((p_1 + q_1/N_1)^2 + (p_2 + q_2/N_2)^2\right)} \right) \end{array}} \\ k_{||} tg\left(\frac{k_{||} l}{2}\right) = \left(\frac{2\pi}{a}\right) \sqrt{\left(p_1 + \frac{q_1}{N_1}\right)^2 + \left(p_1 + \frac{q_1}{N_1}\right)^2} \end{array} \right. \tag{7}$$

Let us note that band gaps (associated with the diffraction of the wave on the lattice of antidots) may appear in the frequencies' spectrum of the investigated spin waves. Such gaps may appear near the edges of the Brillouin zones ($\vec{k}_\perp' = \vec{K}_\perp$), so in these areas of the spectrum the dispersion relation (4) and the spin wave frequencies' spectrum (7) should be refined. For this, let us note that the magnetic potential both inside the film and inside an antidot satisfy the equation $\Delta_\perp \Phi_{0\perp} = -\left(\kappa^2 - \left(\kappa^2 + k_{||}^2\right) f_R(\vec{r}_\perp)\right)\Phi_{0\perp}$ (the function $f_R(\vec{r}_\perp) = \sum_j \chi\left(R - \left|\vec{r}_\perp - \vec{r}_{0j}\right|\right)$ takes into account the periodic structure of the antidots, here χ is the Heaviside function) that is mathematically similar to the two - dimensional Schrödinger equation $\Delta_\perp \psi = -\frac{2m}{\hbar^2}(E - U(\vec{r}_\perp))\psi$ for the electron (with the energy E) wave function ψ in a two - dimensional periodic crystal lattice potential $U(\vec{r}_\perp)$ after the following replacements: $E \to \frac{\hbar^2\kappa^2}{2m}$, $U(\vec{r}_\perp) \to \frac{\hbar^2(\kappa^2 + k_{||}^2)}{2m} f_R(\vec{r}_\perp)$. In the first zone of $k_{||}$ values - where $k_{||}$ is less than or of the same order with κ - a simple model of the theory of crystal solids can be used to take into account this diffraction. Namely, let us make the following replacement (taken from the above-mentioned theory) in the dispersion relation (4) near the boundary of the Brillouin zone:

$$\kappa^2 \to \frac{1}{2}\left(\left(\vec{\kappa}(\vec{k}_\perp')\right)^2 + \left(\vec{\kappa}(\vec{k}_\perp' - \vec{K}_\perp)\right)^2\right) \pm \sqrt{\frac{1}{4}\left(\left(\vec{\kappa}(\vec{k}_\perp')\right)^2 - \left(\vec{\kappa}(\vec{k}_\perp' - \vec{K}_\perp)\right)^2\right)^2 + \left|U_{\vec{K}_\perp}\right|^2} \tag{8}$$

here $U_{\vec{K}_\perp} = \int\limits_{[-a,a)^2} d\vec{r}_\perp \frac{\kappa^2 + k_{||}^2}{a^2} f_R(\vec{r}_\perp) e^{-i\vec{K}_\perp \vec{r}_\perp} = (\kappa^2 + k_{||}^2) B(\vec{K}_\perp)$, $B(\vec{K}_\perp) = \frac{1}{a^2} \int\limits_{|\vec{r}_\perp| \le R} d\vec{r}_\perp e^{-i\vec{K}_\perp \vec{r}_\perp}$ with the substitution of the constant value $\kappa^2 = k_{||}^2 tg^2(k_{||} l/2)$. After some transformations, one can obtain the following expressions in the vicinity of the edge of the first Brillouin zone:

$$\begin{aligned}\omega^2 = \gamma^2 M_0^2 \Bigg(&\left(\alpha^2 (\kappa_1^2 + k_{||}^2)^2 + 2\alpha(2\pi + \tilde{\beta})(\kappa_1^2 + k_{||}^2) + \tilde{\beta}(4\pi + \tilde{\beta}) - 4\pi k_{||}^2 \left(\alpha + \frac{\tilde{\beta}}{\kappa_1^2 + k_{||}^2} \right) \right) \cos^2 \varphi(\vec{k}_\perp') + \\ + &\left(\alpha^2 (\kappa_2^2 + k_{||}^2)^2 + 2\alpha(2\pi + \tilde{\beta})(\kappa_2^2 + k_{||}^2) + \tilde{\beta}(4\pi + \tilde{\beta}) - 4\pi k_{||}^2 \left(\alpha + \frac{\tilde{\beta}}{\kappa_2^2 + k_{||}^2} \right) \right) \sin^2 \varphi(\vec{k}_\perp') \Bigg)\end{aligned} \tag{9}$$

$$\kappa_{1,2}^2 = \left(\frac{\vec{K}_{1,2}^2}{2} + \vec{K}_{1,2}\vec{k}_\perp' + (\vec{k}_\perp')^2 \right) \pm \sqrt{\left(\frac{\vec{K}_{1,2}^2}{2} - \vec{K}_{1,2}\vec{k}_\perp' \right)^2 + k_{||}^4 \left(1 + tg^2\left(\frac{k_{||} l}{2}\right) \right)^2 \left| B(\vec{K}_{1,2}) \right|^2} \tag{10}$$

where $\varphi = arctg\left((k_\perp')_y / (k_\perp')_x\right)$, $\vec{K}_1 = \begin{pmatrix} 2\pi/a \\ 0 \end{pmatrix}$, $\vec{K}_2 = \begin{pmatrix} 0 \\ 2\pi/a \end{pmatrix}$. As a result, the frequency band gap can be written as follows:

$$\Delta\omega = \omega\left(\kappa^2 = \frac{\pi^2}{a^2} + k_{||}^2 \left(1 + tg^2\left(\frac{k_{||} l}{2}\right) \right) \left| B(\vec{K}_{1,2}) \right| \right) - \omega\left(\kappa^2 = \frac{\pi^2}{a^2} - k_{||}^2 \left(1 + tg^2\left(\frac{k_{||} l}{2}\right) \right) \left| B(\vec{K}_{1,2}) \right| \right) \tag{11}$$

For the higher Brillouin zones, the spin wave spectrum near the zones edge can be described by the same relations (9), (10) but with another values of $\vec{K}_{1,2}$ that correspond to the investigated zone.

IV. DISCUSSION

Let us make a graphical representation of the obtained results in the absence of an external magnetic field. Dependence of the spin wave frequency on the longitudinal wave number $k_{||}$ (that implies from the dispersion relation (4) for the Bloch solution taking into account the relation $\kappa = k_{||} tg(k_{||} l/2)$) for l=10 nm is given on the Fig. 2. Dependence of the spin wave frequency on the in-plane wave vector (that implies from the refined relations (9), (10)) for l=10 nm, a=50 nm, R=20 nm (so that the value $\left| B(\vec{K}_{1,2}) \right| \sim 0.4$) for the first interval of values of $k_{||}$ (according to the Fig. 2) and the analogues of the first and the second Brillouin zones are shown on the Fig. 3. Both graphs are plotted for typical values of the ferromagnet parameters (presented in the captions). Numerical estimations for these nanosystem parameters show that the band gap for the boundaries of the first Brillouin zone is approximately $2 \cdot 10^{10}$ Hz. The width of the allowed bands is of the same order of magnitude ($3 \cdot 10^{10}$ Hz).

As it can be seen from the graphs, the values' spectrum of $k_{||}$ contains band gaps. They correspond to the values of $k_{||}$ for which the boundary conditions for the magnetization cannot be satisfied. They are not a classic analogue of the Brillouin band gaps. Their presence causes the values' spectrum of $k_{||}$ to be near discrete one-dimensional $k_{||}(p) = 2\pi p/l$ (with

$p \in \aleph \cup \{0\}$ being a number of the longitudinal mode). As it can be seen from the graph, this approximate discreteness becomes more pronounced with increasing number of the longitudinal mode (branches of the dependence $\omega(k_{\|})$). On the other hand, band gaps in the dependence $\omega(\vec{k}_{\perp}')$ are analogous to the Brillouin band gaps of crystal solids theory. The band gap becomes significant starting from the second longitudinal mode of the dependence $\omega(k_{\|})$, and the spin wave frequencies' spectrum becomes a set of narrow bands. For the first branch, however, one can use the spectrum (7).

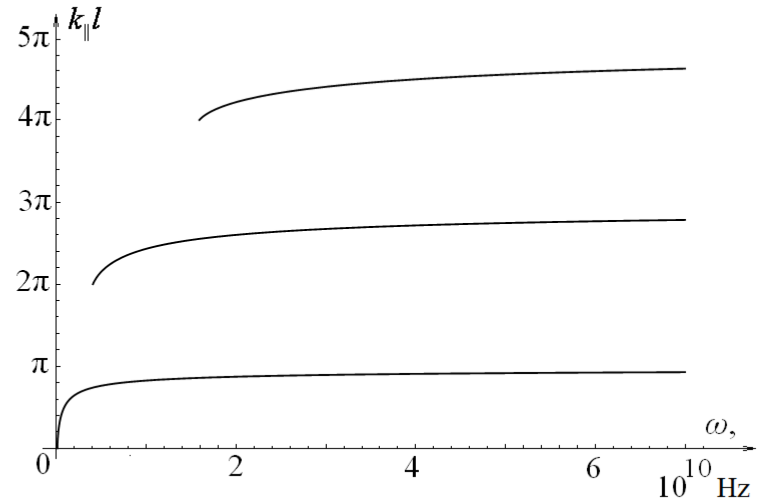

FIGURE 2: Dependence of the spin wave frequency on the longitudinal wavenumber $k_{\|}$ for the following nanosystem parameters: $\alpha=10^{-12}$ cm^{-2}, $\beta=1$, $\gamma=10^{5}$ Hz/Gs, $M_0=10^{3}$ Gs and $l=10$ nm.

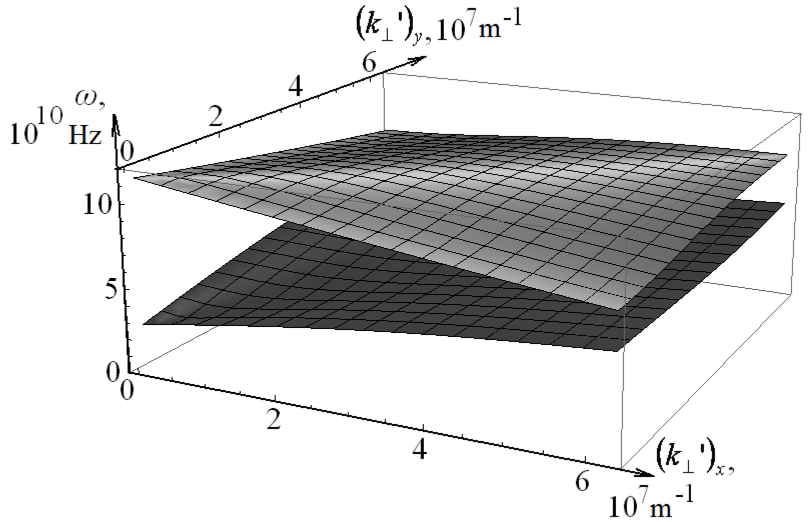

FIGURE 3. Dependence of the spin wave frequency on the in-plane wave vector $\vec{k}_{\perp}'$ for the first branch of the dependence shown on the Fig.2 and the following nanosystem parameters: $\alpha=10^{-12}$ cm^{-2}, $\beta=1$, $\gamma=10^{5}$ Hz/Gs, $M_0=10^{3}$ Gs, $l=10$ nm, $a=50$ nm and $R=20$ nm. The area represented on the graph corresponds to analogues of the first and the second Brillouin zones.

V. CONCLUSION

Therefore, the paper extends the study of the dipole-exchange linear spin waves in a thin ferromagnetic film with a two-dimensional periodic system of identical circular antidots started by the author in the previous paper [10]. The film is assumed to be composed of the uniaxial "easy axis"-type ferromagnet, with the axis of easy magnetization directed orthogonally to the film plane. For such waves, the differential equation for the magnetic potential in the magnetostatic approximation is written. The equation is solved for the case when either the external magnetic field is strong enough or the film is thin enough ($l<<2(a–R)$) to ignore the inhomogeneity of the equilibrium magnetization and magnetic field - and, additionally, the antidots are far enough from each other, so the minimum distance between them is much bigger than the exchange length.

Unlike the previous paper [10], the solution of the Landau-Lifshitz equations for the above-described spin wave in this paper is sought in the form of a two-dimensional function of Bloch type (for the in-plane wave propagation). For such solution, the dispersion relation and the relation between planar and longitudinal wavenumbers are obtained. Then, the crystal solid state formalism is used to obtain the values' spectra of the wave vector components and (after combining with the above-mentioned relations) of the spin waves' frequencies. The obtained results are refined near the edge of the Brillouin zones using the electronic band theory.

It is shown that the values' spectrum of the longitudinal wave numbers has band gaps and is near discrete. It is also shown that a band structure - which is analogous to the electronic band structure of a crystal solid - is inherent for the investigated spin waves.

REFERENCES

[1] Y. Li, W. Zhang, V. Tyberkevych, W. K. Kwok, A. Hoffmann and V. Novosad, "Hybrid magnonics: Physics, circuits, and applications for coherent information processing," J. Appl. Phys., vol. 128, 130902, October 2020.

[2] P. Pirro, V. I. Vasyuchka, A. A. Serga and B. Hillebrands, "Advances in coherent magnonics," Nat. Rev. Mater., vol. 6, pp. 1114-1135, July 2021.

[3] A. Chumak, P. Kabos, M. Wu et al., "Roadmap on spin-wave computing concepts," IEEE Trans. Quantum Eng. (in press, HAL Id: hal-03381543, version 3).

[4] S. Neusser and D. Grundler, "Magnonics: spin waves on the nanoscale," Adv. Mater., vol. 21, pp. 2927–2932, June 2009.

[5] V. V. Kruglyak, S. O. Demokritov and D. Grundler, "Magnonics," J. Phys. D: Appl. Phys., vol. 43, 264001, June 2010.

[6] K. Zakeri, "Magnonic crystals: towards terahertz frequencies," J. Phys.: Condens. Matter, vol. 32, 363001, June 2020.

[7] T. Goto, K. Shimada, Y. Nakamura, H. Uchida and M. Inoue, "One-dimensional magnonic crystal with Cu stripes for forward volume spin waves," Phys. Rev. Appl., vol. 11, 014033, January 2019.

[8] V. V. Kruglyak, R. J. Hicken, A. N. Kuchko and V. Yu. Gorobets, "Spin waves in a periodically layered magnetic nanowire," J. Appl. Phys., vol. 98, 014304, July 2005.

[9] Three-Dimensional Magnonics (ed. by G. Gubbiotti), Jenny Stanford Publishing: New York, 2019, chapter "Spin Waves in Thin Films and Magnonic Crystals with Dzyaloshinskii–Moriya Interactions" by R. A. Gallardo, D. Cortés-Ortuño, R. E. Troncoso and P. Landeros, pp.121-159.

[10] V. V. Kulish, "Spin waves in a ferromagnetic film with a periodic system of antidots,". Journal of nano- and electronic physics, vol. 7, 01020, March 2015.

[11] A. I. Akhiezer, V. G. Baryakhtar and S. V. Peletminskiy, Spin waves, North-Holland: Amsterdam, 1968.

AD Publications

Sector-3, MP Nagar, Bikaner,

Rajasthan, India

www.adpublications.org, info@adpublications.org